J. Membrane Biol. 123, 209–221 (1991)
0022263191001200

The Journal of
Membrane Biology

Diversity of K^+ Channels in the Basolateral Membrane of Resting *Necturus* Oxyntic Cells

Stéphane Supplisson, Donald D.F. Loo, and George Sachs†
Department of Physiology, University of California, School of Medicine, Los Angeles, California 90024-1751, and †Center for Ulcer Research and Education, Wadsworth Veterans Administration Medical Center, Los Angeles, California 90073

Summary. Patch-clamp techniques have been applied to characterize the channels in the basolateral membrane of resting (cimetidine-treated, nonacid secreting) oxyntic cells isolated from the gastric mucosa of *Necturus maculosa*. In cell-attached patches with pipette solution containing 100 mM KCl, four major classes of K^+ channels can be distinguished on the basis of their kinetic behavior and conductance: (1) 40% of the patches contained either voltage-independent (*a*) or hyperpolarization-activated (*b*), inward-rectifying channels with short mean open times (16 msec for *a*, and 8 msec for *b*). Some channels showed subconductance levels. The maximal inward conductance g_{max} was 31 ± 5 pS (n = 13) and the reversal potential E_{rev} was at V_p = −34 ± 6 mV (n = 9). (2) 10% of the patches contained depolarization-activated and inward-rectifying channels with g_{max} = 40 ± 18 pS (n = 3) and E_{rev} was at V_p = −31 ± 5 mV (n = 3). With hyperpolarization, the channels open in bursts with rapid flickerings within bursts. Addition of carbachol (1 mM) to the bath solution in cell-attached patches increased the open probability P_o of these channels. (3) 10% of the patches contained voltage-independent inward-rectifying channels with g_{max} = 21 ± 3 pS (n = 4) and E_{rev} was at V_p = −24 ± 9 mV (n = 4). These channels exhibited very high open probability (P_o = 0.9) and long mean open time (1.6 sec) at the resting potential. (4) 20% of the patches contained voltage-independent channels with limiting inward conductance of 26 ± 2 pS (n = 3) and E_{rev} at V_p = −33 ± 3 mV (n = 3). The channels opened in bursts consisting of sequential activation of multiple channels with very brief mean open times (10 msec). In addition, channels with conductances less than 6 pS were observed in 20% of the patches. In all nine experiments with K^+ in the pipette solution replaced by Na^+, unitary currents were outward, and inward currents were observed only for large hyperpolarizing potentials. This indicates that the channels are more selective for K^+ over Na^+ and Cl^-. A variety of K^+ channels contributes to the basolateral K^+ conductance of resting oxyntic cells.

Key Words K^+ channels · basolateral K^+ conductance · oxyntic cell · acid secretion · patch clamp

Introduction

The oxyntic cell of the gastric mucosa secretes an isotonic solution of HCl in response to various secretagogues. While it is well established that K^+ is essential for secretion (Harris & Edelman, 1960; Berglindh, 1978), the pathways for K^+ across the basolateral and apical membranes and their regulation in resting and stimulated oxyntic cells have not been completely resolved. The basolateral and apical membranes of the oxyntic cell contain two exchange pumps, the electrogenic Na^+, K^+- and the electroneutral H^+,K^+-ATPases that actively transport K^+ into the cell (Ganser & Forte, 1973; Sachs et al., 1976). To maintain K^+ homeostasis K^+ must be recycled across both of these membranes by specific leak pathways. The basolateral membrane of *Necturus* oxyntic cells possesses a high resting K^+ conductance (Blum et al., 1971, Demarest & Machen, 1985) and two classes of K^+ channels, regulated by the second messengers intracellular Ca^{2+} and cAMP, have been identified in this membrane (Ueda, Loo & Sachs, 1987). Cl^- channels, on the other hand, have not been observed in the basolateral membrane of either the oxyntic or the parietal cell. Besides the K^+ channels previously described in the basolateral membrane of the oxyntic cell, there may be others, as it has become apparent in many cells that multiple types of K^+ pathways are involved in ionic and volume homeostasis (for example, *see* Lau, Hudson & Schultz, 1984; Germann, Ernst & Dawson 1986; Butt, Clapp & Frizzell, 1990).

In the present study, we have examined the channels in the basolateral membrane of resting (nonacid-secreting) oxyntic cells, isolated from the *Necturus* gastric mucosa by enzymatic digestion in the presence of the histamine type-2 receptor blocker cimetidine. The results indicate that a variety of K^+ channels with a wide range of kinetic behavior and conductances is present in the basolateral membrane of the resting *Necturus* oxyntic cell.

Materials and Methods

Cell Isolation

Oxyntic cells were enzymatically dissociated from the fundic region of the gastric mucosa of *Necturus* using a procedure modified after Demarest, Loo and Sachs (1989). The tissue, stripped of the underlying muscularis, was incubated for 105 ± 15 min in an isolation medium consisting of a mixture of pronase (Boehringer Mannheim Biochemicals, Indianapolis, IN) and collagenase type IV (Sigma Chemical, St. Louis, MO) each added at 1 mg/ml to an amphibian NaCl Ringer solution (in mM: 85 NaCl, 20 $NaHCO_3$, 5 KCl, 1 $KHPO_4$, 1 $CaCl_2$, 1 $MgCl_2$, 10 HEPES/NaOH at pH 7.3) containing 5 mM D-glucose, 1 mg/ml bovine serum albumin and 0.1 mM cimetidine (Sigma).

After incubation the mucosa was washed with Ringer's solution and any residual mucus was removed with filter paper. The mucosa was kept in an amphibian culture medium (Wolf and Quimby 1964, Gibco Laboratories, Gaithersburg, MD). The oxyntic cells were dispersed from the mucosa by vortexing for 1 min and this cellular suspension was rapidly filtered through a 100 μm diameter nylon mesh. In the amphibian medium the cells and dissociated glands spontaneously clumped and formed a pellet, while vesicles and cellular fragment remained in suspension. The pellet was washed twice in amphibian culture medium, and the cells were kept in this medium either on ice or at room temperature (20°C) for periods of up to 5 hr. Oxyntic cells isolated using this method showed two pronounced differences between those prepared previously using the method of Ueda et al. (1987). The cells are slightly smaller with diameters of approximately 45 μm compared to the previously prepared cells with diameters of 50 μm. The present cells also typically showed a distinctive morphological difference between apical and basolateral membranes. They had a round base and a 'budding' region. Under light microscopy, the region under the nucleus could be identified as the basolateral membrane, while the opposing 'budding' region was the apical membrane (Fig. 1). Oxyntic cells showing this characteristic pattern of differentiation between apical and basolateral membranes were more often observed when animals were maintained in cool water (13°C) for several weeks.

Chemicals and Solutions

During the experiments, the cells were normally bathed in the NaCl Ringer solution described above. The pipette solution contained (in mM): 110 KCl, 1 $MgCl_2$, 1 or 0 $CaCl_2$, 1 or 10 EGTA and 10 HEPES at pH 7.2. Experiments were also performed with the pipette containing NaCl Ringer, Na-gluconate and K-gluconate solutions. The two latter solutions were prepared by substitution of the appropriate Na^+ for K^+ and gluconate for Cl^- in the KCl pipette solution. Tetraethylammonium (10 mM), and quinine (1 mM) were also added to the KCl pipette solution in some of the experiments.

Electrophysiological Methods

Patch pipettes were pulled from Corning 7052 glass and had typical resistances of 10 MΩ. They were placed on the basolateral membrane of the oxyntic cells, identified as described above. With this preparation of oxyntic cells the mean success rate to obtain a gigaseal was 20–25%. Excised patches were difficult to obtain and extremely unstable and all the experiments described in the present study were performed in the cell-attached configuration.

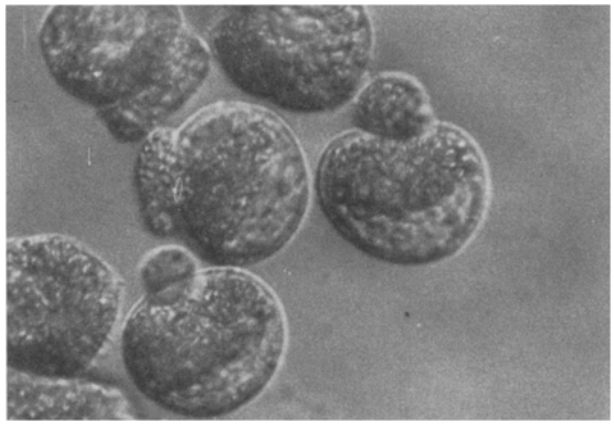

Fig. 1. Morphology of an oxyntic cell isolated from the *Necturus* gastric mucosa in the presence of cimetidine (0.1 mM). This is a photograph of an oxyntic cell viewed under an inverted microscope with Hoffman-modulated optics. The cells showed a round base and a 'budding' region. The region under the nucleus, which we have identified using acridine orange fluorescence, is the basolateral membrane. The 'budding' region expands during acid secretion and is the apical membrane.

All potentials are referred to the bath solution and expressed as pipette potentials V_p. Current-voltage (I-V) relations are plotted according to the usual convention with depolarizing potentials ($-V_p$) to the right of the abscissa. Inward currents, due to cation entry from the pipette into the cell or anion exit from the cell, are represented as downwards deflections of the current records.

All experiments were performed at room temperature (22°C).

Data Analysis

Data were collected and stored in a videocassette system and were digitized using Fetchex program of pClamp (Axon Instruments, Foster City, CA). The current records were first filtered (200 Hz–2 kHz) and then digitized at rates (50 μsec–1 msec), depending on the kinetics of the channels. All the digitized current records were printed out for display and inspection by eye prior to statistical analysis. Current histograms were generated and used to estimate the size of the single channel current steps and the open probability P_o of the channels, which was defined as the fractional open time. For a single channel P_o was determined as the ratio of the area under the current peak over the total area of the histograms (Colquhoun & Sigworth, 1983). The area under each peak was estimated by fitting the total current histogram by nonlinear regression to the sums of multiple Gaussian distributions. However, in the case of rare channel events (less than 5% of the total) or for substates of channels that could not be detected statistically using current histograms, the magnitude of the current steps were read by eye directly using a modified version of Fetchan. Open probability P_o was estimated by determining the sum of the individual single channel openings using

the 50% threshold detection method (Colquhoun & Sigworth, 1983) and dividing by the total time analyzed. For patches that contained multiple channels, the areas under the current histograms was used to estimate P_o, assuming a binomial distribution. For channels of classes 1 (which exhibited subconductance states) and 4 the mean open times were read by eye, whereas for channels of classes 2 and 3 the mean open and closed times were estimated by linear regression of the semilogarithmic plot of their respective frequency histograms. The mean current $\bar{I}$ was obtained by integration of the single channel current per unit of time (*see* legend to Fig. 5*B*). The smooth curves on the current-voltage relationships were drawn by polynomial interpolation.

Statistics are expressed as mean ± SEM.

Results

A total of 162 successful cell-attached patches on the basolateral membrane were obtained. Distinct single channel current steps could be resolved in 83 patches, and this study was based on a partial analysis of 50 records. All the channels observed appeared to be selective for K^+. Their conductance ranged from 3 to 77 pS, and we have been able to classify them into four distinctive classes according to their kinetic properties and conductances:

1) Channels which were either voltage independent [class 1(a)] or hyperpolarization activated [class 1(b)] and exhibited rapid kinetics with brief mean open times (16 msec for class 1(a), and 8 msec for class 1(b)) at the resting potential. The current-voltage relations showed inward rectification with subconductance states.

2) Channels which were activated by depolarizing membrane potentials. With hyperpolarization, these channels showed bursting behavior and exhibited high frequency flickerings.

3) Channels which exhibited slow kinetics with mean open and closed times of 1.6 and 0.2 sec. These channels showed very high activity at the resting potential.

4) Channels which opened in bursts consisting of multiple current levels. These channels showed very rapid kinetic behavior with mean open times of 10 msec, and their activity was independent of voltage.

In addition to these four classes of channels, in 20% of the patches, we observed channels with conductances less than 6 pS. Because of the very small current steps, we were unable to obtain complete *I-V* curves and reliably determine the reversal potentials and the selectivity of these channels.

Class 1: K^+ Channels with Subconductance States and Short Open Times

The most common channel which was observed in 40% of the patches ($n = 20$) showed rapid kinetics of opening and closing, and could be classified into two subtypes: (*a*) voltage independent (60%) and (*b*) hyperpolarization activated (40%). Many of these channels seemed to show subconductance states.

Figure 2*A* shows typical current records for a voltage independent channel with one main conductance and two apparent subconductance levels. Our interpretation that the currents are from a single channel and not from three channels is based on the observations that (i) there were single jumps from the baseline to the second and the main conductance levels, (ii) the sum of the three current levels was not observed, and (iii) the ratio of the maximum to minimum conductance was similar in all the current records from this class of channels. On the other hand, current records that contained multiples of the same current level with fractional open times following the binomial distribution were interpreted as currents from identical independent channels. The mean open time for the channel of Fig. 2*A* was approximately 16 msec at $V_p = 0$ mV. The current-voltage (*I-V*) relations for the three current levels are shown in Fig. 2*B*. The two highest current levels displayed nonlinear *I-V* curves, while that of the lowest level was linear. All three current levels had similar reversal potentials at $V_p = -30$ mV. The limiting conductances for hyperpolarizing potentials (V_p between 40 to 60 mV) were 55, 12 and 9 pS, and in the depolarizing direction (V_p between −80 to −100 mV), the limiting conductances were 8, 6 and 4 pS, respectively. For this class of channels the *I-V* relationship of the largest conductance level always exhibited a pronounced inward rectification, whereas the *I-V* relations of the lowest conductance level was linear. The lowest conductance level was 12 ± 4% ($n = 3$) of the largest level. The limiting conductance in the hyperpolarizing direction (V_p between 40 to 60 mV) ranged from 10 to 61 pS with a mean of 36 ± 9 pS ($n = 6$).

Figure 3*A* shows representative current records for a patch which contained three channels activated by hyperpolarization. At low pipette potentials, for instance, at $V_p = 0$ mV, only one current level (−0.8 pA) could be observed. The mean open time was 8 msec. The number of current levels increased as the membrane was hyperpolarized, and at $V_p = 80$ mV, three current levels are seen—each is a multiple of the lowest level (−3.4 pA).

The *I-V* relations of the single channel current levels are shown in Fig. 3*B*. The relation showed an inward rectification with the limiting conductance of 38 pS for V_p between 80 and 100 mV, and 24 pS for V_p between −40 and −60 mV. The reversal potential was at $V_p = -45$ mV.

The increase in open probability with hyperpolarizing voltages is illustrated in Fig. 3*C* for two

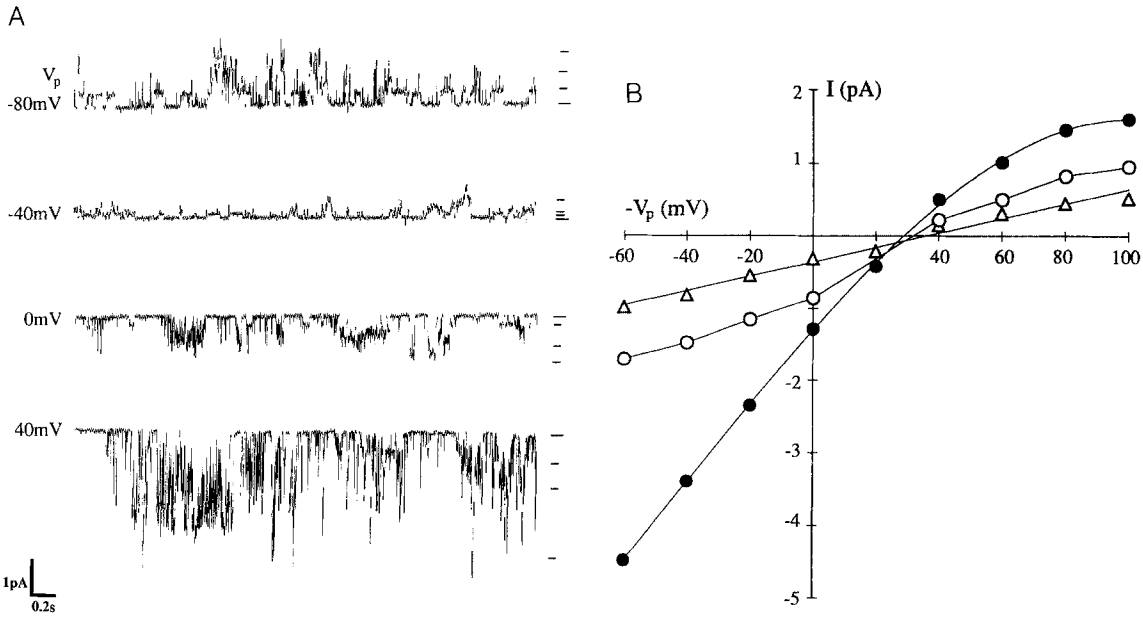

Fig. 2. Current records and *I-V* relationship for a voltage-independent K^+ channel with three conductance states. (*A*) Current records (filtered at 500 Hz) are shown for a channel in a cell-attached patch in the basolateral membrane. Numbers to the left of the traces indicate pipette potentials (V_p). The pipette contained (in mM): 110 KCl, 1 EGTA and 10 HEPES at pH 7.2. (*B*) shows the *I-V* relationship of the three current levels. The limiting conductance in the hyperpolarizing direction (V_p between 40 and 60 mV) was 55, 12 and 9 pS, and in the depolarizing direction (V_p between −80 and −100 mV) was 8, 6 and 4 pS. The reversal potential was $V_p = -30$ mV.

current histograms, at $V_p = 0$ and 80 mV. Increasing the pipette potential from $V_p = 0$ to 80 mV increased the open probability P_o from 0.15 to 0.5. At $V_p = 80$ mV, the areas under the histograms for each of the current levels 0, 1, 2 and 3 were 0.15, 0.34, 0.38 and 0.13, respectively, and are close to the values of 0.13, 0.39, 0.39 and 0.13 predicted by the binomial distribution for $P_o = 0.5$.

In addition to the patches with multiple identical steps (Fig. 3*A*), small conductance substates were also observed for hyperpolarization-activated channels. Apart from their voltage dependence, there was no difference in the maximal inward conductance and the reversal potentials between the voltage-independent and the hyperpolarization-activated channels. The maximal inward conductance and the reversal potentials were 36 ± 9 pS ($n = 6$) and −34 ± 11 mV ($n = 3$) for the voltage-independent channels while the corresponding values for the hyperpolarization-activated channels were 27 ± 5 pS ($n = 7$) and −35 ± 8 mV ($n = 5$). In total the conductance and the reversal potential for all channels of class 2 were 31 ± 5 pS ($n = 13$) and −34 ± 6 mV ($n = 9$).

The reversal potential was in the range of reversal potentials expected for a channel selective for K^+ ions ($V_p = -30$ to −40 mV, assuming a resting membrane potential V_m of −40 mV, Blum et al., 1971; Demarest & Machen, 1985) and an intracellular K^+ concentration of 110 mM), but higher than expected for a channel selective for Cl^- ($V_p = -10$ to −20 mV, assuming an intracellular Cl^- concentration of 30–40 mM).

Class 2: K^+ Channels with Bursting and Flickering Behavior

This class of channels, which was activated by membrane depolarization, was observed in 10% of the records analyzed. The channels opened in bursts for hyperpolarizing potentials, and within each burst the channel openings exhibited a high rate of flicker. Figure 4*A* shows some typical current records for such a channel. The flickering frequency within a burst at the resting potential ($V_p = 0$) was 209 Hz. As the membrane was hyperpolarized, the flickering frequency remained relatively constant and was 210 Hz at $V_p = 20$ mV and 244 Hz at $V_p = 40$ mV. The mean open time increased as the membrane potential was depolarized (*see* Fig. 4*C* below), until for large depolarizations, the channel was virtually open all the time. For instance, at $V_p = -80$ mV, open probability P_o was 0.95.

Single channel *I-V* relationship showed an in-

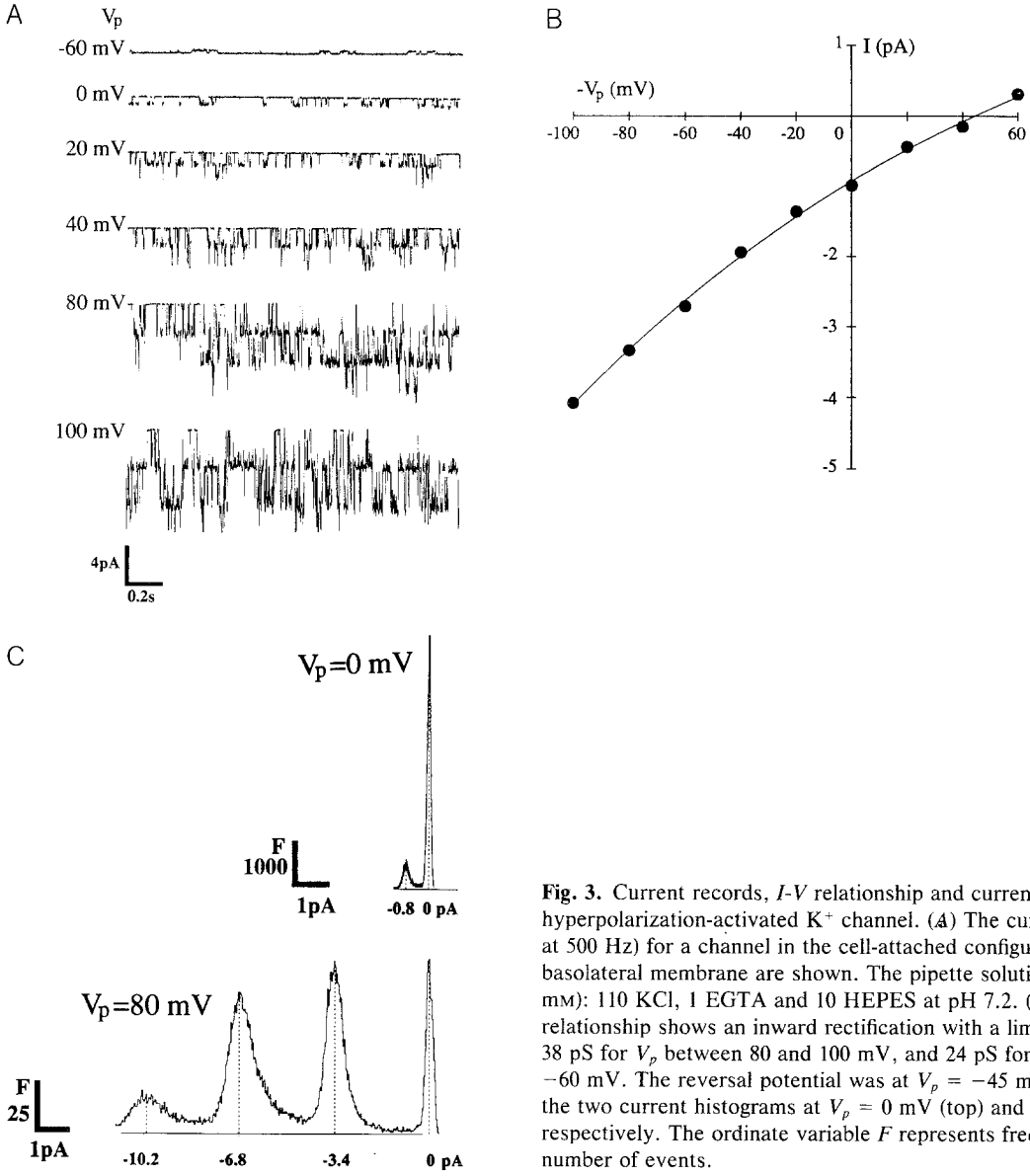

Fig. 3. Current records, *I-V* relationship and current histograms for a hyperpolarization-activated K^+ channel. (*A*) The current records (filtered at 500 Hz) for a channel in the cell-attached configuration in the basolateral membrane are shown. The pipette solution contained (in mM): 110 KCl, 1 EGTA and 10 HEPES at pH 7.2. (*B*) The *I-V* relationship shows an inward rectification with a limiting conductance of 38 pS for V_p between 80 and 100 mV, and 24 pS for V_p between −40 and −60 mV. The reversal potential was at V_p = −45 mV. (*C*) Shown are the two current histograms at V_p = 0 mV (top) and 80 mV (bottom), respectively. The ordinate variable *F* represents frequency or the number of events.

ward rectification (Fig. 4*B*). The limiting conductances were 77 and 23 pS, respectively, in the hyperpolarizing (V_p from 20 to 40 mV) and depolarizing (V_p between −60 to −80 mV) limits. The range of conductances observed for this class of channels was 19–77 pS in the hyperpolarizing direction. The reversal potential was V_p = −39 mV (Fig. 4*B*). In three experiments, the limiting inward conductance was 40 ± 18 pS and the reversal potential was at V_p = −31 ± 5 mV, respectively. This is within the range of reversal potentials for channels selective for K^+.

Figure 4*C* shows the current histograms as a function of pipette potential. Channel open probability P_o showed a large increase with depolarizing membrane potentials. At V_p = 40, 20, 0 and −80 mV, P_o was, respectively, 0.20, 0.20, 0.29 and 0.95. The increase in P_o with depolarizing voltages is due to an increase in the mean open time of the channel. This is illustrated in Fig. 4*D*, which depicts the distribution of the open and close durations of the channel at V_p = 0 and −80 mV. There was no difference in the mean closed times, 2.4 and 2.6 msec. On the other hand, the mean open times increased from 0.5 msec at V_p = 0 mV to 64 msec when V_p = −80 mV.

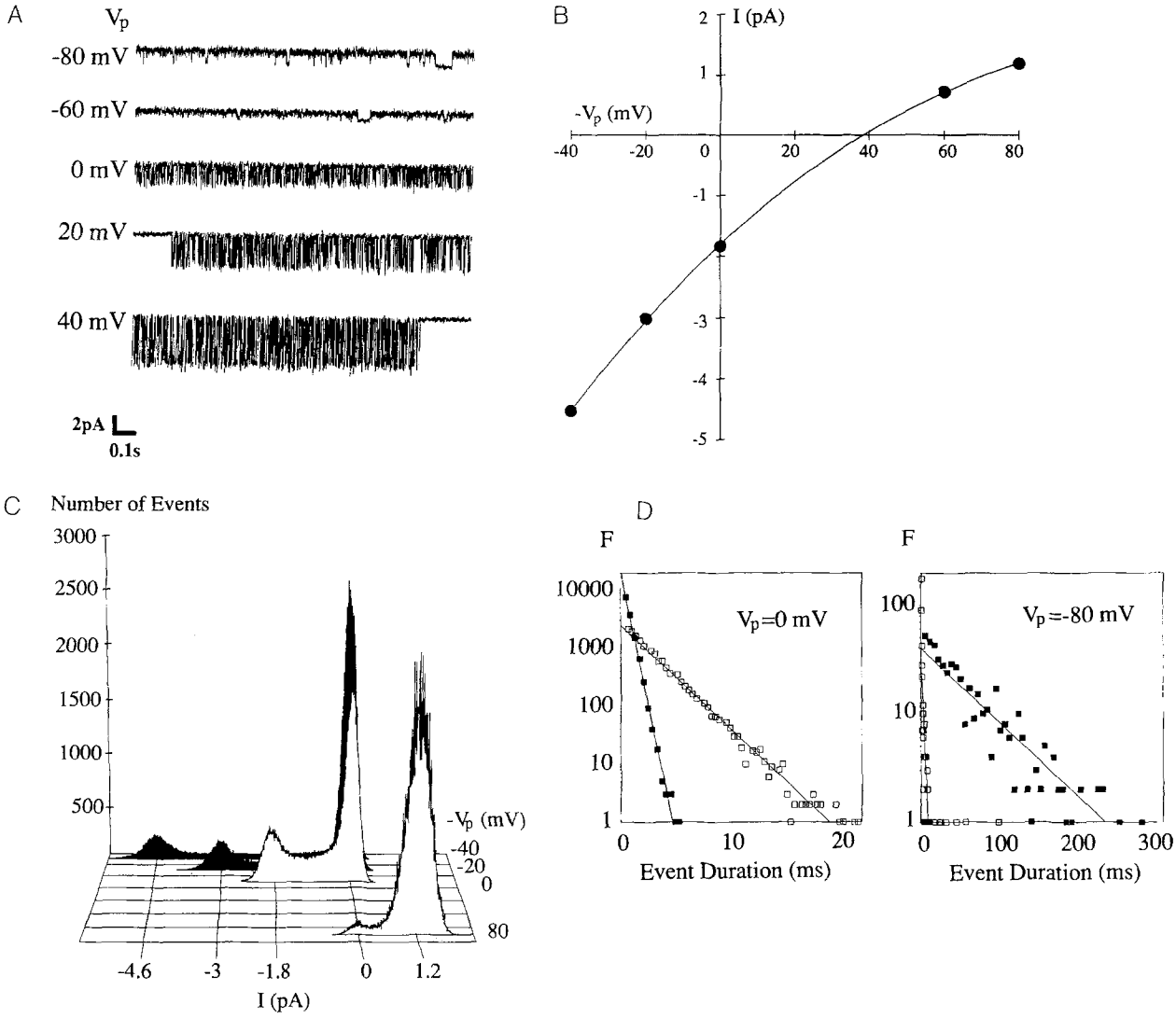

Fig. 4. Current records, *I-V* relationship, and current histograms for a K^+ channel which exhibited bursting and flickering behavior. The experiment was performed in the cell-attached patch configuration. (*A*) The current records, filtered at 1 kHz, are shown. The pipette solution contained (in mM): 110 KCl, 1 EGTA and 10 HEPES at pH 7.2. (*B*) The single channel *I-V* relationship is shown. The limiting conductance in the hyperpolarization direction (V_p between 20 and 40 mV) was 77 pS and in the depolarizing direction (V_p between −60 to −80 mV) was 23 pS. The reversal potential was at $V_p = -39$ mV. (*C*) Shown are the current histograms at four pipette potentials (V_p). The area under the current histograms showed the increase in P_o with depolarizing voltages. Values of P_o, estimated from the 50% threshold-detection method (*see* Materials and Methods), were for V_p of 40, 20, 0 and −80 mV, 0.20, 0.20, 0.29 and 0.95, respectively. (*D*). Semilogarithmic plot is shown of the distribution of the open (filled squares) and closed durations (open squares). Data is shown for two pipette potentials, at $V_p = 0$ and −80 mV. The lines are drawn by linear regression. Slopes for the closed and open durations were: at $V_p = 0$ mV, 2.4 and 0.5 msec, and at $V_p = -80$ mV, 2.6 and 64 msec, respectively.

The pattern of bursting of openings and rapid flickerings within a burst for these depolarization-activated K^+ channels is similar to those described for K^+ channels activated by intracellular Ca^{2+} (Barrett, Magleby & Pallotta, 1982; Moczydlowski & Latorre, 1983). We have examined the effects of carbachol in a cell-attached patch experiment by the addition of the secretagogue to the bath solution. Carbachol has been shown to initiate an increase in intracellular Ca^{2+} in mammalian parietal cells (Muallem & Sachs, 1985; Negulescu & Machen, 1988). Figure 5*A* shows a portion of the continuous current records of a 19-pS channel maintained at $V_p = 0$ mV after the addition of 1 mM carbachol to the bath solution. Stimulation by carbachol resulted in a two fold increase in the open probability P_o (from 0.32 to 0.63 at $V_p = 0$ mV) and a 50% increase in single channel amplitude (from −0.5 to −0.75 pA). The increase in current amplitude would correspond to a 15-mV hyperpolarization of the mem-

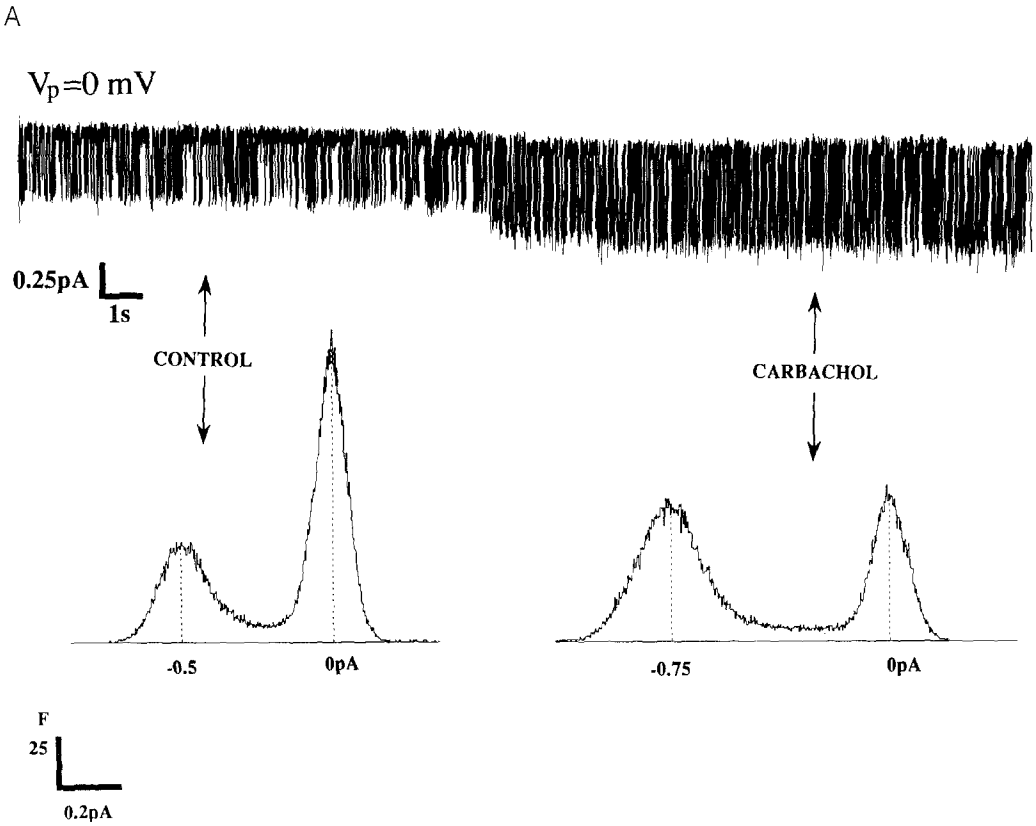

Fig. 5. Activation of a K^+ channel by carbachol. The experiment was performed on a channel (with a limiting inward conductance of 19 pS) in the cell-attached configuration in the basolateral membrane. (*A*) A continuous record of the currents (filtered at 500 Hz) is shown after addition of 1 mM carbachol to the bath solution. The bath solution was continuously perfused. The current histograms indicate that the current amplitudes and open probabilities are: −0.5 pA and 0.32 for the control, and −0.75 pA and 0.63 after carbachol stimulation. The pipette solution contained (in mM): 110 KCl, 1 $MgCl_2$, 10 EGTA, 10 HEPES at pH 7.2, and the bath solution contained NaCl Ringer. (*B*) The complete time course of the mean current $\bar{I}$ is shown, obtained by integration of the single channel current steps per unit of time. The time interval used for integration was 2 sec. The dashed line indicates the baseline prior to carbachol stimulation.

brane potential, assuming carbachol does not affect single channel conductance. This value is in agreement with microelectrode experiments performed in the intact *Necturus* gastric mucosa (Demarest & Machen, 1985). As a result of carbachol stimulation, the mean closed time decreased from 40 to 17 msec, while the mean open time increased slightly from 17 to 25 msec. The time course of the mean current $\bar{I}$ through the channel is shown in Fig. 5*B*. On exposure to carbachol, after a 30-sec delay, $\bar{I}$ increased threefold from −0.16 to −0.47 pA in less than 4 sec and remained constant for several min.

Class 3: Channels with Slow Kinetics and High Activity

Channels with slower kinetics and a very high activity at the resting potential were observed in 10% of

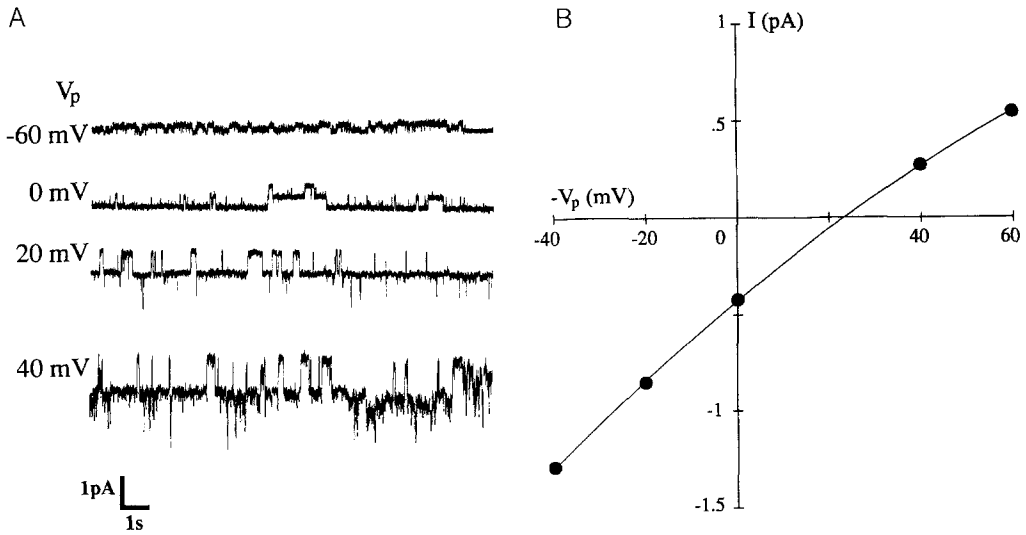

Fig. 6. Current records and *I-V* relations for a K^+ channel which exhibited high activity at the resting potential. (*A*) The current records (filtered at 200 Hz) in the cell-attached configuration are shown. The pipette contained (in mM): 110 KCl, 1 $CaCl_2$, 10 EGTA and 10 HEPES at pH 7.2. The bath solution was NaCl Ringer. (*B*) The *I-V* relationship showed a slight inward rectification with a limiting conductance of 22 pS for V_p between 20 and 40 mV and 14 pS for V_p between −40 and −60 mV. The reversal potential was at $V_p = -25$ mV.

the patches. Figure 6*A* shows the current records for a cell-attached patch containing two such channels which are independent, as the fractional times that 0, 1 and 2 current levels are observed (0.02, 0.19 and 0.79) at $V_p = 0$ mV follow the binomial distribution (with a P_o of 0.87). The mean open and closed times at $V_p = 0$ are 1650 and 240 msec, respectively. We have monitored the activity of the channels continuously for 7 min at the resting potential, and the current histogram indicated that the high open probability ($P_o = 0.92$) is maintained throughout this period. Similar experiments performed in three patches indicated that on the average, P_o was 0.86 ± 0.03 at $V_p = 0$ mV.

The *I-V* relationship for each of the channels of Fig. 6*A* showed a slight inward rectification with a limiting conductance of 22 pS for V_p between 0 and −40 mV, and 14 pS for V_p between −40 and −60 mV (Fig. 6*B*). The reversal potential was at $V_p = -25$ mV. The limiting inward conductance for channels observed in this class ranged from 11 to 26 pS and was 21 ± 3 pS ($n = 4$). The reversal potential was at $V_p = -24 \pm 9$ mV ($n = 4$).

There was no consistent pattern for the voltage dependence of channel activity. For the channel of Fig. 6*A*, P_o was independent of membrane potential in the hyperpolarizing direction (at $V_p = 0$, 20 and 40 mV, P_o was 0.87, 0.88 and 0.84, respectively), and channel activity decreased for depolarizing potentials. However, other channels show their maximal activity at the resting potential ($V_p = 0$ mV) and activity decreased for potentials away from the resting potential.

Class 4: K^+ Channels Exhibiting Bursting Behavior

Channels of this class exhibited bursting behavior. The majority of the patches where we were unable to resolve distinct channel activity contained channels of this class. Patches with distinct current steps were observed in 10 patches (20% of the 50 patches that we have analyzed). These channels were found in association with channels of class 3 in three patches. In most cases, because of their rapid bursting activity, we were unable to perform detailed kinetic analysis on these channels.

Figure 8*A* shows representative current records in a cell-attached patch for a cluster of such channels, the number of current steps could exceed 11. The frequency of bursts did not increase with voltage. However, the size of the burst currents appeared to increase with hyperpolarizing voltages (Fig. 7*A*). At each pipette potential, there were long periods of inactivity of up to several seconds. For instance at $V_p = -40$ mV, the inactive period was longer than 7 sec. The rapid bursts consist of sequential activation of identical multiple channels. These bursts could be longer than 5 sec. Single channel steps could be identified only at the beginning and the end of the bursts. This is illustrated in Fig. 7*B* for another burst of channel openings. The currents at $V_p = 0$ mV are displayed at a shorter time scale, and the individual current steps of 0.5 pA could be observed.

The *I-V* relationship for the discrete current steps of Fig. 7*A* is shown in Fig. 7*C*. The relation

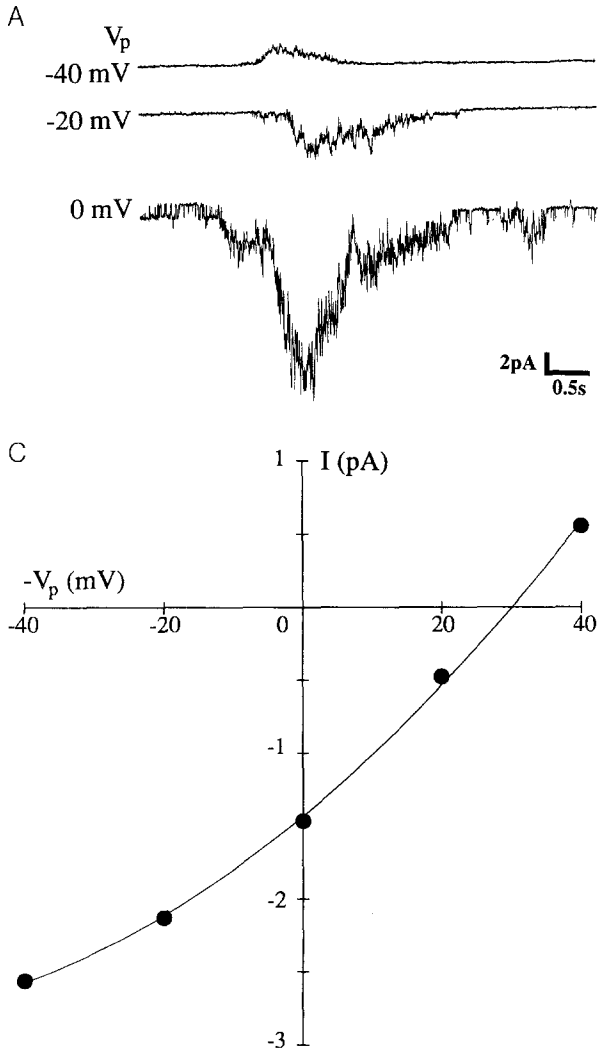

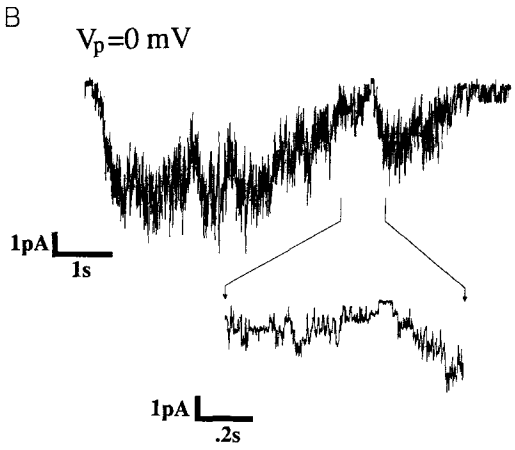

Fig. 7. Current records and *I-V* relationship for a channel which exhibited bursting activity. (*A*) Current records, filtered at 200 Hz, show multiple channels which exhibited rapid bursting kinetics. The pipette solution contained (in mM): 110 KCl, 1 EGTA and 10 HEPES at pH 7.2. (*B*) Representative current records are shown (filtered at 500 Hz) at V_p = 0 mV for a cluster of channels where the individual current steps are discrete during a burst. The time scale is expanded fivefold at the inset, and the multiple current levels are indicated by the dashed lines. In these current records there is a channel from class 4 which is open for most of the time. (*C*) The *I-V* relationship for the discreet current steps of Fig. 8*A* shows an outward rectification with a limiting conductances of 22 and 52 pS in the hyperpolarizing and depolarizing directions (estimated at V_p between 20 and 40 mV, and between +20 and +40 mV, respectively). The reversal potential was at V_p = −30 mV.

showed an outward rectification with limiting inward and outward conductances of 22 pS (for V_p between 20 and 40 mV) and 52 pS (for V_p between −20 and −40 mV). The reversal potential is at V_p = −30 mV. There was no consistent pattern in the rectification of the *I-V* curves for channels in this class. Some channels showed outward rectification (as in Fig. 7*C*), while others showed slight inward rectification (*data not shown*). This may reflect the lack of accuracy in our measurements of the single current steps during bursting activity. In three experiments, the limiting conductance in the hyperpolarizing direction was 26 ± 2 pS. The reversal potential was at V_p = −33 ± 3 mV, and is within the range of reversal potentials for channels selective to K^+ (*see above*).

In three cell-attached patches where pipette solution contained either TEA^+ (10 mM) or quinine (1 mM) which are common blockers of K^+ channels, channels of class 4 were observed, distinguished by their rapid bursting behavior and mean times. We have found no differences in the kinetics and reversal potentials of the channels (*data not shown*).

Experiments with High Na^+ Pipette Solutions

Most of the channels that we have described have reversal potentials in the range expected for channels selective for K^+. Because excised patches were unstable we were unable to test this hypothesis directly, and instead we examined the reversal potential of the channels in cell-attached patches with the pipette K^+ replaced by Na^+. Figure 8*A* shows the current records for a channel in cell-attached configuration with pipette containing NaCl Ringer's solution (105 mM Na^+, 6 mM K^+ and 94 mM Cl^-). This channel most likely belongs to class 1(*a*) because it is voltage independent, the mean open time is 10 msec (at V_p = 0 mV), and the channel does not exhibit any flickerings and bursting ac-

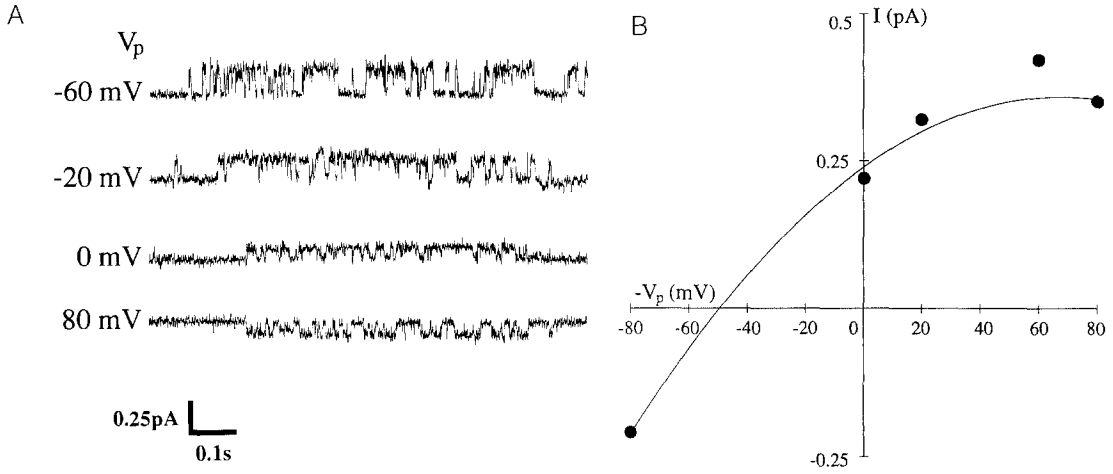

Fig. 8. Current records and *I-V* relationship for a voltage-independent channel in a cell-attached patch when pipette solution contained NaCl Ringer. (*A*) The current records (filtered at 500 Hz) are shown. The pipette solution contained (in mM): 85 NaCl, 20 $NaHCO_3$, 5 KCl, 1 $KHPO_4$, 1 $CaCl_2$, 1 $MgCl_2$ and 10 HEPES/NaOH at pH 7.3. (*B*) *I-V* relations for the channel are shown. The conductances in the hyperpolarizing and depolarizing limits, determined for V_p between 0 and 80 mV and between −20 and −60 mV, were 5 and 2 pS, respectively. The reversal potential was at $V_p = -50$ mV.

tivity. Figure 8*B* shows the *I-V* relationship which exhibited a rectification in the inward direction with a conductance of 6 pS in the hyperpolarizing direction (V_p between 0 and 80 mV) and 2 pS in the depolarizing direction (V_p between −20 to −60 mV). The reversal potential was at $V_p = 50$ mV, and is close to the value of $V_p \approx 40$ mV expected for a channel selective for K^+. Since the calculated reversal potential for Cl^- is in the opposite direction, at $V_p \approx -10$ mV, this indicates that the channel is poorly permeable to Cl^-. The results described in Fig. 8 are typical of all 9 experiments with the pipette solution containing high Na^+. The unitary current steps were outward and always small, less than 0.5 pA, and inward currents were observed only for large hyperpolarizing membrane potentials. The maximal inward conductance level observed in high K^+ pipette solutions (Fig. 2*B*) was not observed when pipette contained high Na^+. The small outward conductance for depolarizing potentials is consistent with the observation that the *I-V* relations of these channels showed inward rectification.

Experiments were also conducted with the pipette Cl^- replaced by gluconate—presumably an impermeant anion. In three experiments with the pipette solution containing 110 mM Na-gluconate (free of K^+ and Cl^-), the currents in cell-attached patches were always outward, and inward currents were not observed for pipette potentials V_p as large as 100 mV (*data not shown*). In six experiments with the pipette solution containing K-gluconate, the conductance and reversal potentials of the channels were in the same range as those obtained with the pipette solution containing KCl. These results are also consistent with the channels being poorly permeable to Na^+ and Cl^-.

In conclusion, in spite of the difficulty of classifying the channels in cell-attached patches, results of the experiments with the pipette solution containing Na^+ indicate that, as a whole, the channels in the basolateral membrane are selective for K^+ and poorly permeable to Na^+ and Cl^-. Because of the very small conductances of the channels observed in cell-attached patches with high Na^+ pipette solutions, we hypothesize that the contribution of the basolateral K^+ channels to whole cell currents in the resting oxyntic cell may be small in normal Ringer's solutions.

Discussion

A variety of experiments, including radiolabeled uptake studies on membrane vesicles prepared from the basolateral membrane of parietal cells (Muallem et al., 1985) and microelectrode experiments on isolated oxyntic cells from the *Necturus* gastric mucosa (Blum et al., 1971) and on oxyntic cells in the intact *Necturus* gastric mucosa (Demarest & Machen, 1985), have shown the presence of a K^+ conductance in the basolateral membrane of resting parietal and oxyntic cells. We have identified at least four classes of K^+ channels in the basolateral membrane of resting oxyntic cells. A summary of their properties is listed in the Table. All the channels showed nonlinear *I-V* relations when pipette solu-

Table. Kinetics of K^+ channels in the basolateral membrane of resting *Necturus* oxyntic cells

Class	Freq (%)	g_{max} (pS)	Range (pS)	E_{rev}[b] (mV)	*I-V* rectification	Voltage activation	Mean open[c] time	Comments
1a	24	36 ± 9(6)	10–61	−34 ± 11(3)	Inward	Independent	16 msec	Subconductance[d]
1b	16	27 ± 5(7)	10–47	−35 ± 8(5)	Inward	Hyperpolarization	8 msec	Subconductance[d]
2	10	40 ± 18(3)	19–77	−31 ± 5(3)	Inward	Depolarization	1 msec	Carbachol-activ.
3	10	21 ± 3(4)	11–26	−24 ± 9(4)	Inward	Independent	1.6 sec	High P_o
4	20	26 ± 2(3)[a]	22–30	−33 ± 3(3)	Inward or outward	Independent	10 msec	Bursts

g_{max} is the maximal conductance in the hyperpolarizing direction.

[a] denotes limiting conductance in the hyperpolarizing direction.

[b] The reversal potential in cell-attached patches. The values are expressed as V_p.

[c] determined at $V_p = 0$ mV.

[d] Indicates that these channels may possess subconductance levels.

The experiments were performed in the cell-attached configuration on the basolateral membrane of resting *Necturus* oxyntic cells. The pipette solution contained 100 mM KCl, and the cells were bathed in NaCl Ringer's solution.

tion contained 100 mM KCl. The range of reversal potentials for the channels showed a wide variation. With the exception of class 3, the reversal potentials are within the range of potentials expected for channels selective for K^+. The reversal potential of class 3 channels was slightly lower, indicating that they may not be as selective for K^+ over Na^+ and/or Cl^-. The conductances of the channels overlapped in the lower conductance range, from 10 to 30 pS. Channels of classes 1(*a*), 3 and 4 are voltage independent, while those of classes 1(*b*) and 2 are activated by hyperpolarizing and depolarizing potentials, respectively. Our classification of the channels according to kinetics and conductance is to some extent arbitrary. In view of the large variations in the kinetic behavior of the channels [for instance, class 3 and between classes 1(*a*) and (*b*)], and the many channels (20%) that were observed with conductances less than 6 pS, there may be more classes of channels than those that we have identified.

Protein modifying agents have been shown to modify channel properties and channel diversity could result from enzymatic modification of K^+ channels during cell isolation. Isolated oxyntic cells are viable and functional as they have resting potentials as high as −60 mV (Demarest, 1991) and respond to stimulation by the secretagogues carbachol and cAMP (present study; Ueda et al., 1987; Demarest et al., 1989). In addition, we have found no consistent pattern in the occurrence of the types of channels between isolated oxyntic cells and oxyntic cells in intact cell clusters which have undergone less enzymatic exposure, and K^+ channels of different classes are commonly observed together in the same patch. Channel diversity is probably a consequence of the physiological requirements of the oxyntic cell rather than the result of channel modification during cell isolation.

The current-voltage relations of all the K^+ channels observed exhibited some degree of rectification. The simplest rectification mechanism is described by the Goldman-Hodgkin-Katz (GHK) equation (*see* Hille (1984) for review) and is due to unequal distribution of K^+ across the membrane. This mechanism is unlikely in our experiments since the pipette $[K^+]$ should be close to the intracellular $[K^+]$. Whether additional complications, such as blockade by intracellular ions (i.e., magnesium), and the properties of the channel itself, could give rise to the rectification observed remains to be determined.

Multiple current levels were observed in many patches, and could be interpreted as arising either from a single channel with subconductance levels (Fig. 2) or from independent channels (Fig. 3). Channels were assumed to be independent if their fractional open times followed the binomial distribution. We have found that some patches contained multiple current levels whose fractional open times obeyed the binomial distribution, and within the analysis period of 20 sec the activity of the channels appeared to be stationary. In one patch containing channels of class 1(*b*) we were able to examine the activity for longer periods (≈10 min). For all voltages, we noticed that the channels appeared to be activated in periodic bursts with a mean period τ of 156 ± 6 sec ($n = 9$). This period is similar to the oscillations of membrane potential ($\tau = 124 \pm 8$ sec) recently described in isolated *Necturus* oxyntic cells by Demarest (1991).

Two K^+ channels have previously been described in the basolateral membrane of *Necturus* oxyntic cells: a 65-pS depolarization-activated

channel regulated by $[Ca^{2+}]_i$ (K_{Ca} channel) and a 33-pS voltage-independent channel regulated by intracellular cAMP (Ueda et al., 1987). Both channels exhibited linear *I-V* relationships in cell-attached patches. Recently, Mieno et al. (1990) have also found two K^+ channels of similar conductance and regulation in the basolateral membrane of bullfrog oxyntic cells: a 56-pS channel activated by $[Ca^{2+}]_i$ and a 28-pS channel activated by intracellular cAMP. However, both channels exhibited inward rectification and were not observed in nonstimulated cells. Our observations agree with those of Mieno et al. (1990) in that the *I-V* curves of the basolateral K^+ channels are nonlinear. We have shown that channels of class 2 are activated by carbachol and hence presumably intracellular Ca^{2+} (Muallem & Sachs, 1985; Negulescu & Machen, 1988). In addition to the rectification of the *I-V* curves, these channels also exhibited a narrower range of conductance (19–77 pS) compared to the K_{Ca} channels (45–145 pS). Large conductance "maxi-K" channels were not observed in the present study.

The common occurrence and voltage independence of class 1(*a*) channels suggest that they may be cAMP-activated. But intracellular cAMP is probably very low in cimetidine-treated cells and one would expect cAMP-regulated channels to be inactive. Thus it is likely that these could represent a different class of K^+ channels. Sakai et al. (1989) have observed inward rectifying K^+ channels in the basolateral membrane of rabbit parietal cells. These channels, which they found in three out of 877 patches (0.3%), had a conductance of 230 pS under symmetrical high K^+ conditions and were not activated by either cAMP nor Ca^{2+}.

Multiple subtypes K^+ channels appear to be a common phenomenon in a variety of cells. More than six distinct types of K^+ channels have been found in the apical membrane of the rabbit corneal endothelium (Rae, Levis & Eisenberg, 1988). Butt et al. (1990) have found that the basolateral membrane of canine tracheal epithelium possesses three distinct K^+ conductance pathways. One of these K^+ conductance pathways was induced by cell swelling. It appears that in a variety of tissues distinctive classes of K^+ channels may be involved in separate regulatory tasks.

There are several possible physiological roles for K^+ channels in the oxyntic cell: (i) The basolateral membrane of the oxyntic cell contains a large K^+ conductance, and the resting potential of the basolateral membrane is very close to the K^+ equilibrium potential (Demarest & Machen, 1985). This resting K^+ conductance is presumably involved in the recycling of K^+ pump into the cell by the Na^+, K^+-ATPase. (ii) Gastric juice contains up to 15 mM KCl (Makhlouf, 1981), and therefore the oxyntic cell is being depleted of KCl during secretion. Maintenance of $[K]_i$ is performed by the Na^+, K^+-ATPase and K^+ channels in the basolateral membrane, the H^+, K^+-ATPase and a KCl exit pathway in the apical membrane. With stimulation by either the Ca^{2+}- or cAMP-mediated second messenger system, in event of an imbalance between the influx and efflux of K^+, the activation of basolateral K^+ channels which is selectively responsive to each of these second messenger systems may be necessary (Ueda et al., 1987). (iii) With secretion, there may be additional requirements for K^+. One example relates to the osmotic effect of ion movement from either surface of the cell. Unless the resting and secretory states are perfectly matched, the efflux of K^+ and Cl^- from either side of Cl^--secreting epithelia will result in either loss or gain of KCl with accompanying H_2O, and subsequent cell shrinkage or swelling. The loss of KCl from the apical membrane of the parietal cell and K^+ from the basolateral membrane surface will also result in cell shrinkage, and basolateral K^+ channels are likely to be involved in the compensatory response. Finally, (iv) K^+ channels may be involved in the secretion of pepsinogen by the oxyntic cell.

This study is the first part of a comprehensive study to characterize the whole cell currents in the oxyntic cell under resting and stimulated conditions. The results indicate that a number of K^+ channels contribute to the resting basolateral K^+ conductance, and the basolateral K^+ conductance of the resting oxyntic cell may be small when bathed in NaCl Ringer's solution. This provides the background information for identification of the K^+ currents in the resting oxyntic cell.

This work was supported by NIH grant DK40615 and a U.S. Veterans Administration Senior Medical Investigator Award to G.S. We thank Drs. Ernest M. Wright and Lucie Parent for their helpful comments on the manuscript.

References

Barrett, J.N., Magleby, K.L., Pallotta, B.S. 1982. Properties of single calcium-activated potassium channels in cultured rat muscle. *J. Physiol.* **331**:211–230

Berglindh, T. 1978. The effects of K^+ and Na^+ on acid formation in isolated gastric glands. *Acta Physiol. Scand.* **Spec. Suppl.:** 55–68

Blum, A.L., Shah, G.T., Wiebelhaus, V.D., Brennan, F.T., Helander, H.F., Ceballos, R., Sachs, G. 1971. Pronase method for isolation of viable cells from *Necturus* gastric mucosa. *Gastroenterology* **61**:189–200

Butt, A.G., Clapp, W.L., Frizzell, R.A. 1990. Potassium con-

ductances in tracheal epithelium activated by secretion and cell swelling. *Am. J. Physiol.* **258:**C630–C638

Colquhoun, D., Sigworth, F.J. 1983. Fitting and statistical analysis of single-channel records. *In*: Single-Channel Recording. B. Sakmann and E. Neher, editor. pp. 191–263. Plenum, New York

Demarest, J.R. 1991. Potassium channel-dependent membrane potential oscillations in oxyntic cells. *Biophys. J.* **59:**649 (*abstr.*)

Demarest, J.R., Loo, D.D.F., Sachs, G. 1989. Activation of apical chloride channels in the gastric oxyntic cell. *Science* **245:**402–404

Demarest, J.R., Machen, T.E. 1985. Microelectrode measurements from oxyntic cells in intact *Necturus* gastric mucosa. *Am. J. Physiol.* **23:**C535–C540

Ganser, A.L., Forte, J.G. 1973. K^+-stimulated ATPase in purified microsomes of bullfrog oxyntic cells. *Biochim. Biophys. Acta* **307:**169–180

Germann, W.J., Ernst, S.A., Dawson, D.C. 1986. Differentiation of two distinct K conductances in the basolateral membrane of turtle colon. *J. Gen. Physiol.* **88:**237–252

Harris, J.B., Edelman, I.S. 1960. Transport of potassium by the gastric mucosa of the frog. *Am. J. Physiol.* **198:**280–284

Hille, B. 1984. Ionic channels of excitable membranes. Sinauer, Sunderland (MA)

Latorre, R., Oberhauser, A., Labarca, P., Alvarez, O. 1989. Varieties of calcium-activated potassium channels. *Annu. Rev. Physiol.* **51:**385–399

Lau, K.R., Hudson, R.L., Schultz, S.G. 1984. Cell swelling increases a barium-inhibitable potassium conductance in the basolateral membrane of *Necturus* small intestine. *Proc. Natl. Acad. Sci. USA* **81:**3591–3594

Makhlouf, G.M. 1981. Electrolyte composition of gastric secretion. *In*: Physiology of the Gastrointestinal Tract. L.R. Johnson, editor. pp. 551–566. Raven, New York

Mieno, H., Shirakawa, T., Inoue, M., Kajiyama, G. 1990. Patch-clamp studies of K^+ channels in frog oxyntic cells. *Gastroenterology* **98:**A548 (*abstr.*)

Moczydlowski, E., Latorre, R. 1983. Gating kinetics of Ca^{2+}-activated K^+ channels from rat muscle incorporated into planar lipid bilayers. Evidence for two voltage-dependent Ca^{2+}-binding reactions. *J. Gen. Physiol.* **82:**511–542

Muallem, S., Burnham, C., Blissard, D., Berglindh, T., Sachs, G. 1985. Electrolyte transport across the basolateral membrane of the parietal cell. *J. Biol. Chem.* **260:**6641–6653

Muallem, S., Sachs, G. 1985. Ca^{2+} metabolism during cholinergic stimulation of acid secretion. *Am. J. Physiol.* **248:**G216–G228

Negulescu, P.A., Machen, T.E. 1988. Intracellular Ca regulation during secretagogue stimulation of the parietal cell. *Am. J. Physiol.* **254:**C130–C140

Rae, J.L., Levis, R.A., Eisenberg, R.S. 1988. Ionic channels in ocular epithelia. *In*: Ion Channels. Vol 1, pp. 283–327. T. Narahashi, editor. Plenum, New York

Sachs, G., Chang, H.H., Rabon, E., Schackmann, R., Lewin, M., Saccomani, G. 1976. A nonelectrogenic H^+ pump in plasma membrane of hog stomachs. *J. Biol. Chem.* **251:**7690–7698

Sakai, H., Okada, Y., Morii, M., Takeguchi, N. 1989. Anion and cation channels in the basolateral membrane of rabbit parietal cells. *Pfluegers Arch.* **414:**185–192

Ueda, S., Loo, D.D.F., Sachs, G. 1987. Regulation of K^+ channels in the basolateral membrane of *Necturus* oxyntic cells. *J. Membrane Biol.* **97:**31–41

Received 18 October 1990; revised 14 February 1991